What Happens to Molecules as They React? A Valence Bond Approach to Reactivity

Sason S. Shaik

Contribution from the Department of Chemistry, Ben-Gurion University of the Negev, P.O.B. 653, Beer Sheva, 84120, Israel. *Received June 12, 1980*

Abstract: A methodology for conceptualization and construction of potential energy curves for a variety of organic reactions is presented. We suggest that in all reactions which involve covalent bond-making and bond-breaking steps, the ground potential energy curve arises from an intersection of two curves—one which is initially a ground configuration and the other an excited configuration which contains the VB "image" of the product. The curve crossing turns out to be a heuristic electronic promotion which prepares the closed shell reactants for bond reorganization. It may also be described as a switchover of two VB structures, one reactant-like, the other product-like. This behavior is shown to be general whenever at least one of the reactants is closed shell. Examples are given for nucleophilic, electrophilic, and symmetry-forbidden reactions.

What happens to molecules as they react? In most cases, reactants have to traverse a barrier after which they are transformed to products. Different reactions may differ in the intimacies of their reaction surfaces, yet they all, more or less, conform to this general scheme; a barrier has to be traversed before the reaction system can rest in the energy well of the products.

What do we know about the mechanism of barier formation? The pioneering studies of Woodward and Hoffmann[1] and of Longuet-Higgins and Abrahamson[2] have shown that the barrier in the so-called forbidden reactions arises from the avoided or intended crossing of two surfaces, one of which is initially a diexcited state. The origins of this were attributed to the orbital crossing imposed by symmetry constraints. Thus, it is known as a "symmetry-imposed barrier".[3]

Slowly, one is led to recognize that *avoided crossing*[4] *could be a general mechanism whereby molecules rearrange their electrons, so that some bonds can be broken and others, new ones, formed.*[5]

What we are after is the topology of this electronic reorganization during the chemical transformation of reactants to products.

Our strategy of attacking the problem is by fusing the insights of MO theory, LCFC[6-8] (a localized reactant configuration approach), and the valence bond (VB) approach.

Scheme I. Ground and Excited Reactant Configurations for the Description of Nucleophilic Attacks

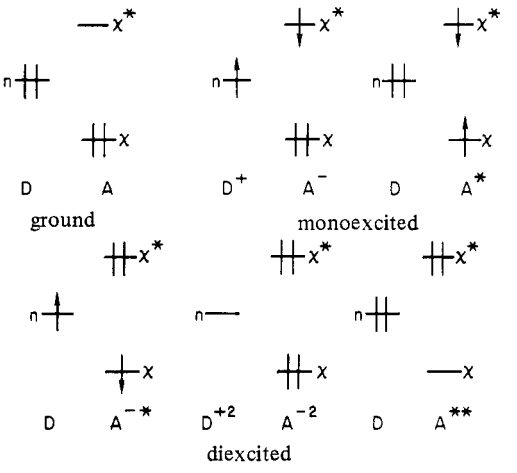

As a starting point we shall consider the *adiabatic* potential energy curve arising from an MO-CI treatment. More intimate information will be unravelled as we shall trace the reactant configurations which intersect to yield the adiabatic curve.[9,10] VB analysis will complete the intimacy of this information. It will lead to a view of reactivity in terms of the crossing of VB structures.

No doubt, the reader will recognize much of the strategy underlying our approach. It constitutes a natural evolution of the interest, our[6] and others,[1-5,7,9,10] in potential energy surfaces of organic reactions. The time, we believe, has arrived when the quantum mechanical insight into the chemical behavior of organic molecules can be translated into a generality which provides an answer to the question: what is common to thermal organic reactions which involve simultaneous bond-breaking and bond-making steps?

(1) (a) Woodward, R. B.; Hoffmann, R. *J. Am. Chem. Soc.* **1965**, *87*, 395, 2511. (b) Hoffmann, R.; Woodward, R. B. *Ibid.* **1965**, *87*, 2046, 4388.

(2) Longuet-Higgins, H. C.; Abrahamson, E. W. *J. Am. Chem. Soc.* **1965**, *87*, 2045-2046.

(3) For a summary see: Woodward, R. B.; Hoffmann, R. "The Conservation of Orbital Symmetry"; Academic Press: New York, 1970.

(4) The notion and theory of surface crossing can be dated back to the 1920's. Some of the leading references are: (a) von Neumann, J. Wigner, E. P. *Z. Phys.* **1929**, *30*, 467. (b) Teller, E. *J. Chem. Phys.* **1937**, *41*, 109-116. (c) O'Mally, T. F. *Adv. Atom. Mol. Phys.* **1971**, *7*, 223-249. (d) Carrington, T. *Acc. Chem. Res.* **1974**, *7*, 20-25. (e) Razi Naqvi, K. *Chem. Phys. Lett.* **1972**, *15*, 634.

(5) The role of avoided surface crossing in photochemical organic reactions is described by: (a) Van der Lugt, W. Th. A. M.; Oosterhoff, L. J. *J. Am. Chem. Soc.* **1969**, *91*, 6042-6049. (b) Dougherty, R. C. *Ibid.* **1971**, *93*, 7187-7201. (c) Michl, J. *Ibid.* **1971**, *93*, 523. (d) Michl, J. *Mol. Photochem.* **1972**, *4*, 243-255, 257-286, 287-314. (e) Michl, J. *Top. Curr. Chem.* **1974**, *46*, 1. (f) Michl, J. *Pure Appl. Chem.* **1975**, 507-534. (g) Michl, J. *Photochem. Photobiol.* **1977**, *25*, 141-154. (h) Gerhartz, W.; Poshusta, R. D.; Michl, J. *J. Am. Chem. Soc.* **1976**, *98*, 6427-6443. (i) *Ibid.* **1977**, *99*, 4263-4271. (j) Salem, L.; Dauben, W. G.; Turro, N. J. *J. Chim. Phys. Physicochim. Biol.* **1973**, *70*, 694. (k) Salem, L. *J. Am. Chem. Soc.* **1974**, *96*, 3486-3501. (l) Salem, L.; Leforestier, C.; Segal, G.; Wetmore, R. *Ibid.* **1975**, *97*, 479-487. (m) Dauben, W. G.; Salem, L.; Turro, N. J. *Acc. Chem. Res.* **1975**, *8*, 41-54. (n) Salem, L. *Science*, **1976**, *191*, 822-830. (o) Devaquet, A. *Pure Appl. Chem.* **1975**, *41*, 455-473.

(6) For the use of this approach to the discussion of potential energy surfaces in organic reactions, see: (a) Epiotis, N. D.; Shaik, S. In "Progress in Theoretical Organic Chemistry"; Csizmadia, I. G., Ed.; Elsevier: Amsterdam, 1977; Vol. 2. (b) Epiotis, N. D.; Shaik, S. *J. Am. Chem. Soc.* **1977**, *99*, 4936-4946. (c) Epiotis, N. D.; Shaik, S. *Ibid.* **1978** *100*, 1-8, 9-17, 29-33. (d) Shaik, S.; Epiotis, N. D. *Ibid.* **1978**, *100*, 18-29. (e) Epiotis, N. D.; Shaik, S.; Zander, W. In "Rearrangements in Ground and Excited States"; De Mayo, P., Ed.; Academic Press: New York, 1980. (f) Shaik, S. S. *J. Am. Chem. Soc.* **1979**, *101*, 3184-3196. (g) Epiotis, N. D. "Theory of Organic Reactions"; Springer-Verlag: Heidelberg, 1978. (h) Epiotis, N. D. *Pure Appl. Chem.* **1979**, *51*, 203-231.

(7) The donor-acceptor formalism was first introduced by Mulliken, see: (a) Mulliken, R. S. *J. Am. Chem. Soc.* **1952**, *74*, 811-824. (b) Mulliken, R. S. *J. Phys. Chem.* **1952**, *56*, 801-823. (c) Mulliken, R. S.; Person, W. B. "Molecular Complexes"; Wiley-Interscience: New York, 1969.

(8) Much of the development, refinement, and application of the approach is due to the work of Fukui's group, see: (a) Fukui, K.; Fujimoto, H. *Bull. Chem. Soc. Jpn.* **1968**, *41*, 1989-1997. (b) Fukui, K. *Top. Curr. Chem.* **1970**, *15*, 1. (c) Fukui, K. "Theory of Orientation and Stereoselection"; Springer-Verlag: Heidelberg, 1975. (d) Fujimoto, H.; Fukui, K. In "Chemical Reactivity and Reaction Paths"; Klopman, G., Ed.; Wiley: New York, 1974, pp 23-54.

(9) Such crossings were invoked in aromatic substitution by: (a) Brown, R. D. *J. Chem. Soc.* **1959**, 2224-2232. (b) Nagakura, S. *Tetrahedron Suppl. 2* **1963**, *19*, 361-377.

(10) Similar crossings were invoked for the photochemical reactions of carbonyl, see: (a) Maharaj, U.; Csizmadia, I. G.; Winnik, M. A. *J. Am. Chem. Soc.* **1977**, *99*, 946-948. (b) Devaquet, A.; Sevin, A.; Bigot, B. *Ibid.* **1978**, *100*, 2009-2011.

0002-7863/81/1503-3692$01.25/0

We would like to propose here that if one uses reactant configurations as one's basis, one can derive a basic principle for all such thermal organic reactions. Based on this qualification, reaction surfaces result from the intersection of two main reactant configurations—one initially a ground configuration and the other an excited configuration. This rule arises from the basic nature of the chemical process bond making accompanied by bond breaking.

I. Theory

The central question is how do organic molecules combine to form products? To attempt to fully answer this question may be overly ambitious. Therefore, we shall focus on one class of reactions and try to discover the underlying principles behind the transformation of reactants to products. With these at hand, we can proceed to different classes and attempt to gain an insight into the principles governing other chemical transformations, with an aim to find some general behavior.

Our treatment will focus on ground surfaces. The nature of the excited surfaces will be only lightly touched upon and will await a more deserving treatment in the future.

Let us consider a reaction in which a nucleophile (D) attacks a substrate (A). During the process a new bond is formed between D and A, while a bond in A is being cleaved. Reactions of this kind, among others, are nucleophilic substitutions on tetrahedral carbon (reaction 1) or nucleophilic additions to an unsaturated system (reaction 2).

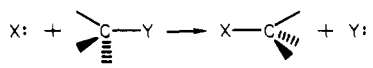

(1)

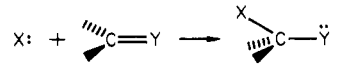

(2)

Y = O, CH_2, etc.

In order to simplify the analysis, let us assume at the outset that, to a first approximation, we can consider only the frontier orbitals of the reactants, which are a high lying filled orbital (n) of D and a pair of bonding and antibonding orbitals (χ and χ^*) of A. Limiting ourselves to these MOs, we can write the different wave functions (ground and excited) of the system as a linear combination of the reactant configurations which arise by distributing the four reacting electrons among the three orbitals n, χ, and χ^*.[6-8] This is strictly correct as long as one has a way of defining these orbitals within the delocalized orbitals of the complex *at each point along the reaction surface*. There are six configurations of this type and they are shown in Scheme I below, organized according to their order of excitation with respect to the reactants. Thus the DA configuration, sometimes called "no-bond",[6,7] is a ground configuration according to this definition, while the charge transfer (D^+A^-) and the locally excited (DA*) configurations are monoexcited with respect to the initial configurations of the reactants, etc.

The reactant configurations are expressed as linear combinations of Slater determinants—the closed shell configurations by one determinant and the open shell ones by two determinants. For example, DA reads

$$DA = \frac{1}{1 - S_{n\chi}^2}(4!)^{-1/2}|n\bar{n}\,\chi\bar{\chi}| \tag{3}$$

where the barred orbitals are β spin orbitals and the unbarred ones denote α spin orbitals. The terms in front of the determinant grouped together are the normalization constant, where $S_{n\chi}$ is the MO overlap between n and χ. The appearance of the latter in the normalization constant occurs whenever we do not neglect overlap (see supplementary material for details).

An example for an open shell configuration is D^+A^-, reading

$$D^+A^- = [2(1 - S_{n\chi}^2 + S_{n\chi^*}^2)]^{-1/2}(4!)^{-1/2}\{|\chi\bar{\chi}\,n\bar{\chi}^*| - |\chi\bar{\chi}\,\bar{n}\chi^*|\} \tag{4}$$

The reader should note that the term open shell should not be taken to mean that we are dealing with diradicals. The two odd electrons are *spin paired* (Scheme I) and constitute together what we would call a *bond pair*. As we shall see later, this bond pair is responsible for the intermolecular bonding effected during the chemical transformation.

Since the wave functions which we are using as our basis are localized reactant configurations, they will help us to follow "what happens" to the reactants as they react. For example, one may find that the wave function of the reaction complex changes its main character from DA to one of the excited reactant configurations in Scheme I. Then one talks about an avoided crossing of these two configurations followed by changes in the electronic nature of the reactants. This avoided crossing will usually leave its memory as a barrier on the reaction surface.

In discussing possible intersection of reactant configurations, one can express the various states (Ψ_i) of the reaction complex as a linear combination of these configurations, i.e.,

$$\Psi_i = c_{1i}DA + c_{2i}D^+A^- + c_{3i}DA^* + c_{4i}D^+A^{-*} + c_{5i}DA^{**} + c_{6i}D^{+2}A^{-2} \tag{5}$$

Alternatively, one can perform MO calculations buttressed by CI, so that some or all of the correlation effects can be taken into account, and then expand the MO–CI wave function in terms of these configurations, i.e.,

$$\Psi_i(\text{MO–CI}) = c_{1i}DA + c_{2i}D^+A^- + \ldots \tag{6}$$

In view of the accessibility of MO calculations, this second approach is much easier. It also has more pedagogical value, since it effectively illustrates the parts-to-the-whole relationship between the localized configurtional wave function (eq 5) and the delocalized MO–CI wave functions (eq 6). Ultimately, one can carry this expansion all the way to valence bond (VB) structures[11] and hope to achieve better insight into the nature of curve crossing and electronic reorganization.

Let us demonstrate our ideas on a prototype reaction

$$H{:}^- + H{-}H \rightarrow H{-}H + {:}H^- \qquad (H{:}^- \equiv D;\ H{-}H \equiv A) \tag{7}$$

The MOs of the reaction complex H_3^- can be calculated with any available MO method along some points of the reaction coordinate. Then, one computes the MOs of the fragments at the same geometry as they appear in the reaction complex. This allows one to express the MOs of the complex in terms of the MOs of the fragments (n, σ, and σ^*).[12]

$$\phi_1 = a_1n + b_1\sigma - c_1\sigma^* \qquad \phi_2 = a_2n - b_2\sigma - c_2\sigma^* \qquad \phi_3 = -a_3n + b_3\sigma - c_3\sigma^* \qquad a, b, c > 0 \tag{8}$$

This is nothing else but an explicit expression of what one knows as the interaction diagram.[12] The signs of the orbital mixings can be simply rationalized by using perturbation arguments as invoked by the Hoffmann group.[12] The interaction diagram is shown in Figure 1. One can see that aside from the mixing of n into σ and σ^*, the latter two mix with each other indirectly via n. The sign of this mixing is given by the second-order perturbation expression.[13] For example, σ^* mixes into σ with a negative sign since

$$\frac{S_{n\sigma}S_{n\sigma^*}}{(\epsilon_\sigma - \epsilon_n)(\epsilon_\sigma - \epsilon_{\sigma^*})} < 0$$

(11) VB expansion of MO wave functions is described by: (a) Goddard, W. A., III; Dunning, T. H., Jr.; Hunt, W. J.; Hay, P. J. *Acc. Chem. Res.* **1973**, *6*, 368–376. (b) Alston, P. V.; Shillady, D. D.; Trindle, C. *J. Am. Chem. Soc.* **1975**, *97*, 469–476. (c) Hiberty, P. C.; Leforestier, C. *Ibid.* **1978**, *100*, 2012–2017. (d) Slater, J. C. *J. Chem. Phys.* **1965**, *43*, 811. (e) Mulliken, R. S. *Phys. Rev.* **1932**, *41*, 49. (f) Berry, R. S. *J. Chem. Phys.* **1959**, *30*, 936. (g) Harcourt, R. D.; Harcourt, A. *J. Chem. Soc., Faraday Trans. 2* 1974, *70*, 743. (h) Harcourt, R. D. *Int. J. Quantum Chem.* **1973**, *4*, 173. (i) Hirst, D. M.; Linnet, J. W. *J. Chem. Phys.* **1965**, *43*, 874.

(12) This method has been used for some time by the Hoffmann group to analyze structure and reactivity problems. Some representative papers are: (a) Hoffmann, R. *Acc. Chem. Res.* **1971**, *4*, 1–9. (b) Hoffmann, R. *Pure Appl. Chem.* **1971**, *2*, 233–250. (c) Hoffmann, R. *Ibid.* **1971**, *28*, 181–194. (d) Elian, M.; Hoffmann, R. *Inorg. Chem.* **1975**, *14*, 1058–1076.

(13) Libit, L.; Hoffmann, R. *J. Am. Chem. Soc.* **1974**, *96*, 1370–1383.

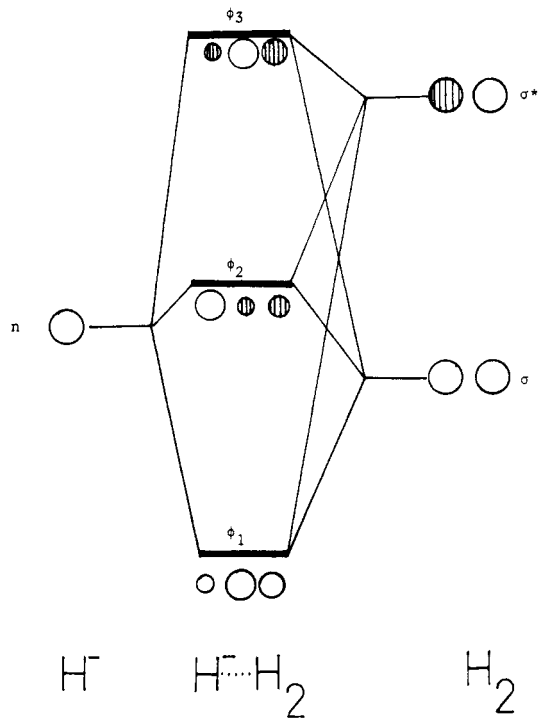

Figure 1. Interaction diagram for the reaction $H^- + H_2$. n, σ, and σ^* are the RMOs of H^- and H_2, respectively. ϕ_1, ϕ_2, and ϕ_3 are the delocalized MOs of $H^- \ldots H_2$.

Accordingly, ϕ_1 (eq 8) will be composed of σ mixing into itself n with a positive sign, and σ^* with a negative sign. The net result is the so-called polarization of σ which becomes unbalanced so as to increase its bonding with the incoming H (Figure 1). Similarly, ϕ_2 arises from n combining σ in an antibonding fashion and σ^* in a bonding fashion.[14]

Once one knows the various coefficients in eq 8, one can project out the coefficient of each fragment configuration from the MO wave function and then check the effect of MO–CI on this coefficient. The details of this algorithm are given in the supplementary material deposited with this paper.

Let us give here one example. The coefficient of DA, $c_0(DA)$, within the ground MO wave function, $\Psi_0 = N|\phi_1\bar{\phi}_1\phi_2\bar{\phi}_2|$, is (see eq 8 and Figure 1):[15]

$$c_0(DA) = (1 - S_{n\sigma}^2)\begin{vmatrix} a_1 & a_2 \\ b_1 & -b_2 \end{vmatrix}^2 = (1 - S_{n\sigma}^2)(a_1b_2 + a_2b_1)^2 \quad (9)$$

In general, all the coefficients of the reactant configurations are determinants whose raws are the reactant MO(RMO) coefficients (a_i, b_i, c_i) in the appropriate delocalized MOs (ϕ_1, ϕ_2, and ϕ_3). Thus, for DA, the raws are the coefficients of the n RMO in ϕ_1 and ϕ_2 (a_1, a_2) and the coefficients of σ in the same orbitals (b_1, $-b_2$).

One can now take any MO wave function and obtain the relative weights of the reactant configurations within it. The trends would be similar, regardless of the level of sophistication of the MO computations, since one is using the MO coefficient and not MO energies. For example, simply by inspecting eq 8 and Figure 1, one can conclude that the sum of products ($a_1b_2 + a_2b_1$) should decrease as H^- approaches H_2, since σ^* mixes increasingly more into n and σ and its weights, c_1 and c_2, in ϕ_1 and ϕ_2 increase. Hence, $c_0(DA)$ in eq 9 decreases along the reaction coordinate.

In order to illustrate this, let us start with the ϕ_1, ϕ_2, and ϕ_3 MOs obtained by neglect of AO overlap. These MOs can be easily derived for three points along the reaction coordinate: at infinite (or long) $H^- \cdots H_2$ separation, at some point where the forming and the breaking bonds are equally distant from the middle H, and at a point where the new bond is fully formed and the old one fully broken. This allows us to obtain the coefficients a_i, b_i, and c_i ($i = 1, 2, 3$) in eq 8. Clearly, at first $\phi = \sigma$, $\phi_2 = n$, and $\phi_3 = -\sigma^*$ (Figure 1),[14] so that $b_1 = a_2 = c_3 = 1$. Thus, the coefficient of DA in the ground MO wave function, Ψ_0, is: $c_0(DA) = 1$. At the final point, ϕ_1 becomes the σ orbital of the new bond and, therefore, $a_1 = 1/\sqrt{2}$, $b_1 = 1/2$ and $c_1 = 1/2$. The arithmetics involved in obtaining these coefficients is illustrated pictorially in eq 10. Following identical reasoning for ϕ_2 and ϕ_3,

$$\phi_1 = \frac{1}{\sqrt{2}}(\odot + \odot\!\!-\!\!\cdot) = \frac{1}{\sqrt{2}}(\odot) + 0.5\left(\frac{1}{\sqrt{2}}[\odot\!\!-\!\!\odot + \odot\!\!-\!\!\bullet]\right) \quad (10)$$

one obtains that $a_2 = 0$, $b_2 = 1/\sqrt{2}$, and $c_2 = 1/\sqrt{2}$, while $a_3 = 1/2$, $b_3 = 1/2$, and $c_3 = 1/2$. Thus, $c_0(DA) = 0.25$ (eq 9) at the reaction final point.

We can further refine this result by examining the effect of the doubly excited MO configurations, $\Psi_{2d} = N_2|\phi_1\bar{\phi}_1\phi_3\bar{\phi}_3|$ and $\Psi_{3d} = N_3|\phi_2\bar{\phi}_2\phi_3\bar{\phi}_3|$. These MO wave functions differ from Φ_0 each by two spin orbitals and, hence, they mix with it only via the electron–electron repulsion terms (bielectronic terms) of the Hamiltonian.[16] The bielectronic terms are always positive and consequently Ψ_{2d} and Ψ_{3d} mix into Ψ_0 with a negative sign. Thus, the ground wave function is described by $\sim(1/(1 + \lambda_1^2 + \lambda_2^2)^{1/2})\{\Psi_0 - \lambda_1\Psi_{2d} - \lambda_2\Psi_{3d}\}$, the λs being mixing coefficients.

At the reaction starting point, $\phi_1 = \sigma$, $\phi_2 = n$, and $\phi_3 = -\sigma^*$, and hence $\Psi_{3d} = DA^{**}$ and $\Psi_0 = DA$. Therefore, at the beginning, the ground state of the complex is mainly DA with a small contribution from DA^{**}.[17]

We have seen that as the reaction proceeds the coefficient of DA in Ψ_0 decreases, reaching 0.25 at the reaction final point. Mixing of Ψ_{2d} and Ψ_{3d} into Ψ_0 will further decrease this coefficient. The coefficients of DA within Ψ_{2d} and Ψ_{3d} are

$$c_2(DA) = (1 - S_{n\sigma}^2)\{a_1b_3 + b_1a_3\}^2 \quad (11)$$

$$c_3(DA) = (1 - S_{n\sigma}^2)\{a_2b_3 + b_2a_3\}^2 \quad (12)$$

At the reaction final point they become $c_2(DA) = 0.5$ and $c_3(DA) = 0.25$. Since $c(DA) \simeq (1/(1 + \lambda_1^2 + \lambda_2^2)^{1/2})\{c_0(DA) - \lambda_1c_2(DA) - \lambda_2c_3(DA)\}$, the weight of DA in the ground state diminishes, reaching near zero at the product state.

The result is clear-cut; one starts with a ground state wave function which is mainly DA and ends up with a wave function which contains almost no DA.

What happens then is clearly some sort of avoided crossing. One surface, which is described mainly by DA, is being intersected by another surface which is described by one or more of the excited reactant configurations in Scheme I. In order to find out the surface(s) which cross to define the product, we have performed

(14) The sign of σ^* in ϕ_2 is negative since $S_{n\sigma^*} < 0$, owing to the sign convention used for σ^* in Figure 1. The sign of this mixing will be reversed if the AO signs of σ^* are reversed.

(15) This type of algorithm was described before by Fukui and Fujimoto see: (a) Fujimoto, H.; Hoffmann, R. *J. Phys. Chem.* **1974**, *78*, 1167–1173. (b) Fujimoto, H. Inagaki, S. *J. Am. Chem. Soc.* **1977**, *99*, 7424–7432. (c) Fujimoto, H.; Osamura, Y. Minato, T. *Ibid.* **1978**, *100*, 2954–2959. (d) Kato, S.; Fujimoto, H.; Yamabe, S.; Fukui, K. *Ibid.* **1974**, *96*, 2024–2029. (e) Fujimoto, H.; Kato, S.; Yamabe, S.; Fukui, K. *J. Chem. Phys.* **1974**, *60*, 572–578.

(16) Rules for taking matrix elements between two configurations are given inter alia in: McGlynn, S. P.; Vanquickenborne, L. G.; Kinoshita, M.; Carroll, D. G. "Introduction to Applied Quantum Chemistry"; Holt, Rinehart and Winston: New York, 1972, pp 281–298. The matrix elements of Ψ_0 with Ψ_{2d} and Ψ_{3d} are: $\langle\Psi_0|\mathcal{H}|\Psi_{2d}\rangle = \langle\phi_2\phi_3|1/r_{ij}|\phi_2\phi_3\rangle = K_{23} > 0$ and $\langle\Psi_0|\mathcal{H}|\Psi_{3d}\rangle = \langle\phi_1\phi_3|1/r_{ij}|\phi_1\phi_3\rangle = K_{13} > 0$. The mixing coefficients are: $\lambda_1 = |K_{23}/\{E(\Psi_0) - E(\Psi_{2d})\}|$ and $\lambda_2 = |K_{13}/\{E(\Psi_0) - E(\Psi_{3d})\}|$.

(17) This mixing is identical with the mixing of $|\sigma^*\bar{\sigma}^*|$ into $|\sigma\bar{\sigma}|$ in the case of an isolated H_2 molecule. Upon mixing, part of the zwitterionic VB component (H^+H^-: and H^-: H^+) is being deleted, making the bond more covalent (i.e., H·· H): $(1/(1 + \lambda^2)^{1/2})\{|\sigma\bar{\sigma}| - \lambda|\sigma^*\bar{\sigma}^*|\} = 1/(2(1 + \lambda^2))^{1/2}[(1 + \lambda)\{|S_1\bar{S}_2| - |\bar{S}_1S_2|\} + (1 - \lambda)\{|S_1\bar{S}_1| + |S_2\bar{S}_2|\}]$. See the lucid discussions in: (a) Salter, J. C. "Quantum Theory of Molecules and Solids"; McGraw-Hill: New York, 1963; Vol. 1 Chapters 3 and 4. (b) Salem, L.; Rowland, C. *Angew. Chem., Int. Ed. Engl.* **1972**, *11*, 92–111. (c) See also ref 11a and others cited therein.

Table I. Coefficients of Reactant Configurations in Ψ_0, Ψ_{2d}, and Ψ_{3d} (Obtained by Neglect of AO Overlap in the MOs) for the Model Reaction 7

config	H $\overset{r_1}{\longleftrightarrow}$ H $\overset{r_2}{\longleftrightarrow}$ H MO wave function	coefficients[a,b] R	I	P
DA	Ψ_0	1	+0.729	+0.250
	Ψ_{2d}	0	+0.250	+0.500
	Ψ_{3d}	0	+0.020	+0.250
D^+A^-	Ψ_0	0	−0.604	−0.500
	Ψ_{2d}	0	+0.500	0
	Ψ_{3d}	0	+0.103	+0.500
DA*	Ψ_0	0	+0.177	+0.354
	Ψ_{2d}	0	+0.354	−0.707
	Ψ_{3d}	0	+0.177	+0.354
D^+A^-*	Ψ_0	0	+0.103	+0.500
	Ψ_{2d}	0	+0.500	0
	Ψ_{3d}	0	−0.604	−0.500
DA**	Ψ_0	0	+0.021	+0.250
	Ψ_{2d}	0	+0.250	+0.500
	Ψ_{3d}	1	+0.729	+0.250
$D^{+2}A^{-2}$	Ψ_0	0	+0.250	+0.500
	Ψ_{2d}	1	+0.500	0
	Ψ_{3d}	0	+0.250	+0.500

[a] R ($r_1 = \infty$; $r_2 = 0.75$ Å); I ($r_1 = r_2$); P ($r_1 = 0.75$ Å; $r_2 = \infty$). [b] The expression for the coefficients is discussed in the supplemental material. Note, the coefficient of each configuration, i, is $\sim 1/\{1 + \lambda_1^2 + \lambda_2^2\}^{1/2}\{C_0(i) - \lambda_1 C_2(i) - \lambda_2 C_3(i)\}$. The λ's are mixing coefficients of Ψ_{2d} and Ψ_{3d} into Ψ_0. See eq 11 and 12 and the following discussion.

the complete analysis of all the configurations for the three geometric points of interest: R (reactants), I (intermediate), and P (products), discussed before. The results for the neglect of AO overlap wave functions are shown in Table I.

If one follows the evolution of the coefficients in Ψ_0, one finds that at the reactant geometry (R), Ψ_0 is purely DA. At some intermediate geometry (I), which is taken to represent a possible transition state having equal degrees of bond formation and bond cleavage, the coefficient of DA drops, becoming roughly equal to that of D^+A^-. At this geometry (I), the other reactant configurations contribute much less than the two principal configurations, DA and D^+A^-. At the final point, the product geometry (P), c(DA) becomes small and the products are described by a pack of excited reactant configurations, headed by D^+A^- and D^+A^-*.

If one considers the effect of Ψ_{2d} and Ψ_{3d}, one finds the same trend. At the initial geometry, R, the wave function is mainly DA mixed with some DA**.[17] At the final point, P, DA almost vanishes *and the products are described by the pack of the excited reactant configurations headed again by D^+A^- with an equal amount of D^+A^-* and smaller amounts of the rest of the reactant configurations.*

This behavior can be anticipated. We will come back to it later and show that it stems from simple topological considerations. Right now, we wish to complete the picture and trace the origins of the excited reactant configurations in the various states of the reactants. Table I already reveals some of the information; the diexcited configurations, $D^{+2}A^{-2}$ and DA**, are the ancestors of the doubly excited MO configurations Ψ_{2d} and Ψ_{3d}. What about D^+A^-, DA*, and D^+A^-*? These configurations do not appear in Ψ_0, Ψ_{2d}, and Ψ_{3d} at the initial geometry, R (Table I). Therefore, one must trace them among the remaining MO wave functions Ψ_1, Ψ_4, and Ψ_5, which are shown below:

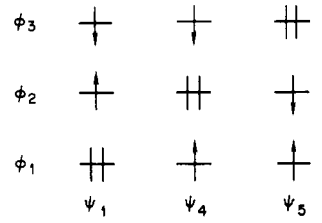

Ψ_1 is the lowest excited MO configuration of the complex, whereas the others are higher lying excited MO configurations. Our analysis shows that at the reactant's geometry, R, $\Psi_1 = D^+A^-$, $\Psi_4 = DA^*$, and $\Psi_5 = D^+A^-$*.

The first excited state of the complex is not described by a single MO configuration. It arises from mixing of Ψ_{2d}, Ψ_{3d}, Ψ_4, and Ψ_5 into Ψ_1.[18] Thus, the first excited state of the complex, at geometries close to R, is described by the pack of the excited reactant configurations (Scheme I) headed by D^+A^-.

Now the picture is clearer; *the surface which intersects with DA is originally the first excited surface of the reaction complex, with D^+A^- being its leading reactant configuration.* As we shall see later the significance of D^+A^- in the intended crossing is not accidental.

The conclusions we have just reached are not dependent on the level of the MO computations. They will carry over to any method based on MO description. Tables II and III summarize the results of the same analysis for MO wave functions obtained by an ab initio SCF–MO method and by the Extended Hückel (EH) method, respectively.

In the ab initio computations the intermediate point, I, corresponds to what was reported as the transition state in the reaction $H^- + H_2 \rightarrow H_2 + H^-$.[19]

The results are virtually identical and the trend in both Tables is the same as predicted from the neglect of AO overlap MOs in Table I. That is, at the transition state, DA and D^+A^- are the principal reactant configurations (Table II) with roughly equal coefficients: $c(DA) \approx (1/(1 + \lambda_1^2)^{1/2})\{0.620 - \lambda_1(0.468)\}$ and $c(D^+A^-) \simeq (-1/(1 + \lambda_1^2 + \lambda_2^2)^{1/2})\{0.410 + \lambda_1(0.774) + \lambda_2(0.243)\}$. On the other hand, at the initial geometry, R, the ground state is mainly DA whereas at the products' geometry, P, DA almost disappears ($c(DA) \approx (1/(1 + \lambda_2^2)^{1/2})\{0.122 - \lambda_2(0.583)\}$) and the pack of excited reactant configurations, led by D^+A^- and D^+A^-*, describes the ground state of the products (see footnote c in Table II).

In summary, as H^- attacks H_2, avoided crossing occurs between one surface which is initially a ground state (DA) and another which is initially an excited state (D^+A^-). This avoided crossing is described schematically in Figure 2.[20]

In the intermediate geometry, I, the avoided crossing is primarily between DA and D^+A^-. These two configurations differ by one spin orbital and hence they interact via one electronic matrix element. This one can be set proportional to the overlap of the reactant orbitals n and σ* (i.e., the HOMO and the LUMO) which differ in the occupancy of one electron in the two configurations (see supplementary material):[6-8]

$$\langle DA|\mathcal{H}|D^+A^-\rangle = 2(4!)N_{DA}N_{D^+A^-}\langle n|\hat{\mathcal{H}}|\sigma^*\rangle \approx kS_{n\sigma^*} \quad (13)$$

The extent of avoided crossing is twice this matrix element. Its memory is retained as a barrier on the ground surface and as an intermediate or a "hole"[5-8] (only at weakly avoided crossing cases) on the excited surface. At the locus of avoided crossing, the ground and the excited states can be described as hybrids of DA and D^+A^-. The smaller contributions of other configurations are omitted:

$$\text{ground} \approx 1/\sqrt{2}\{DA - D^+A^-\} \equiv \text{transition state} \quad (14)$$

$$\text{excited} \approx 1/\sqrt{2}\{DA + D^+A^-\} \equiv \text{intermediate ("hole")} \quad (15)$$

Figure 2b implies that the forward and the reverse reactions are treated differently. This is of course not so; it arises because the products are expressed in terms of reactant configurations. This will become clearer in section II as we will interpret the config-

(18) This mixing again is due to bielectronic terms as discussed in ref 16.
(19) Keil, F.; Ahlrichs, R.; *J. Am. Chem. Soc.* **1976**, *98*, 4787–4793.
(20) Note the similarity of our curves to the Bell–Evans–Polanyi curves, see: (a) Bell, R. P. *Proc. R. Soc. London., Ser. A* **1936**, *A154*, 414. (b) Evans, M. G.; Polanyi, M. *Trans. Faraday Soc.* **1938**, *34*, 11. (c) Ogg, R. A., Jr.; Polanyi, M. *Ibid.* **1935**, *31*, 604. (d) Warhurst, E. *Q. Rev. (London).* **1951**, *5*, 44. (e) See also: Laidler, K.; Shuler, K. E. *Chem. Rev.* **1951**, *48*, 153–224.

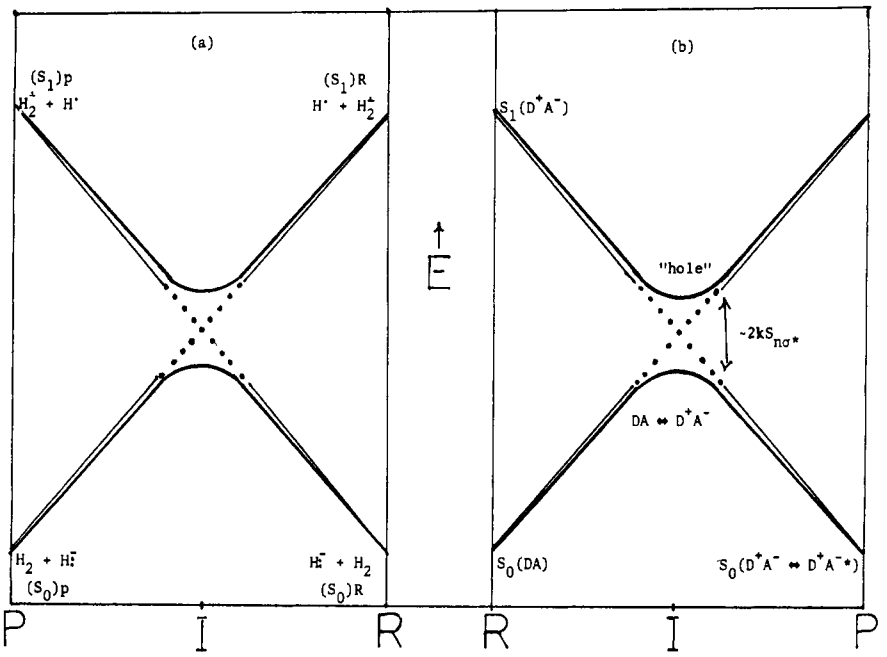

Figure 2. (a) Schematic representation of the curve crossing for the reaction $H^- + H_2 \rightarrow H_2 + H^-$. R, I, P are reactant, intermediate, and product geometries, respectively. The reactant configurations are shown by thin lines and the adiabatic curves by thick lines. The avoided crossing is indicated by circles. The ground state of the reactant, $(S_0)_R$, becomes the excited state of the product, $(S_1)_P$, and conversely. (b) General representation of the curve crossing in terms of reactant configurations. The transition state is DA ↔ D^+A^- and above it there is an intermediate, or possibly a "hole" in the excited surface. The product is described in terms of reactant configurations as roughly D^+A^- ↔ D^+A^{-*}. The contribution of other configurations is omitted.

Table II. Coefficients of Reactant Configurations for $H^- + H_2$ in Ψ_0, Ψ_{2d}, and Ψ_{3d}, Using STO-3G MOs

	coefficients[a,b]		
config	R	I	P[c]
DA	1.000 (0, 0)	0.620 (0.468, 0.047)	+0.122 (+0.705, +0.583)
D^+A^-	0 (0, 0)	−0.410 (0.774, 0.243)	−0.304 (+0.006, +1.463)
D^+A^{-*}	0 (0, 0)	0.125 (0.463, −1.061)	+0.300 (+0.006, −1.437)
DA*	0 (0, 0)	0.203 (−0.401, 0.292)	+0.177 (−1.027, 0.843)
$D^{+2}A^{-2}$	0 (1.000, 0)	0.117 (0.562, 0.554)	+0.302 (0.000, +1.459)
DA**	0 (0, 1.000)	0.035 (0.169, 0.897)	+0.120 (+0.708, +0.577)

[a] $H_1 \leftarrow r_1 \rightarrow H_2 \leftarrow r_2 \rightarrow H_3$; R ($r_1 = \infty$, $r_2 = 0.75$ Å); I ($r_1 = r_2 = 1.0845$ Å); P ($r_1 = 0.75$ Å; $r_2 = \infty$). [b] In parentheses, coefficients in Ψ_{2d} and Ψ_{3d}, respectively. AO overlap is included. [c] Note, the coefficient of $D^{+2}A^{-2}$ at the P geometry is very small, $c(D^{+2}A^{-2}) \approx (1/(1 + \lambda_2^2)^{1/2})\{0.302 - \lambda_2(1.459)\}$, and those of D^+A^- and D^+A^{-*} are large, $c(D^+A^-) \approx (-1/(1 + \lambda_2^2)^{1/2})\{0.304 + \lambda_2(1.463)\}$ and $c(D^+A^{-*}) = (1/(1 + \lambda_2^2)^{1/2})\{0.300 + \lambda_2(1.437)\}$.

Table III. Coefficients of Reactant Configurations in $\Psi_0(\phi_1^2\phi_2^2)$ for $H^- + H_2$, Using EH MOs

	coefficients[a,b]		
coefficient	R	I	P
DA	0.99953	0.66900	0.13000
D^+A^-	−0.01244	−0.49200	−0.31600
D^+A^{-*}	~0.00000	+0.07200	+0.29800
DA*	~0.00000	+0.13700	+0.17900
DA**	~0.00000	+0.01400	+0.11600
$D^{+2}A^{-2}$	~0.00000	+0.17600	+0.30100

[a] $H \leftarrow r_1 \rightarrow H \leftarrow r_2 \rightarrow H$; R ($r_1 = 3$ Å; $r_2 = 0.75$ Å); I ($r_1 = r_2 = 1.5$ Å); P ($r_1 = 0.75$ Å; $r_2 = 3$ Å), AO overlap is included. [b] The coefficients in Ψ_{2d} and Ψ_{3d} are not shown; when included the results are vitually the same as in Table II. Even for the intermediate point, *I*, $c(DA) \approx (1/(1 + \lambda^2)^{1/2})\{0.669 - \lambda_1(0.330)\}$ and $c(D^+A^-) = (-1/(1 + \lambda_1^2 + \lambda_2^2)^{1/2})\{0.492 + \lambda_1(0.595) + \lambda_2(0.157)\}$ which are very close to the coefficients in Table II.

urations in terms of VB structures.

Now we come back to our original question: what happens to H^- and H_2 as they react? We know that the wave function of the system changes from DA to D^+A^- and then to a combination of D^+A^- and D^+A^{-*}. The effect of these changes on the reactants can be illustrated by inspecting the population of the reactant MOs n, σ, and σ* along the reaction coordinate at the three points of interest, R, I, and P. The results are shown in Table IV They

Table IV. Electronic Population in the Reaction MOs (RMOs) during the Reaction $H^- + H_2 \rightarrow H_2 + H^-$

	population[a,b]		
RMO	R	I	P
σ*	0.00042	0.53675	1.47934
σ	2.00000	1.95050	1.52012
n	1.99958	1.51275	1.00054

[a] The results are based on EH calculations. Only Ψ_0 is analyzed. [b] The geometries R, I, and P are specified in Table III.

illustrate the increasing population in σ* on account of the corresponding decrease in population in n and σ. At the intermediate geometry, representing the transition state, there is a net transfer of ~0.5 e from n to σ*, while σ retains its original density, ~2 e. This is analogous to the description of the transition state as a hybrid of DA and D^+A^- (eq 16), thus leading to average populations of 1.5 e and 0.5 e for n and σ*, respectively.

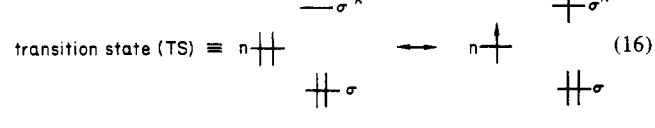

(16)

At the product geometry, P, 1 e has been tansferred from n to σ*. In addition, 0.5 e shifts from σ to σ*. This compliments

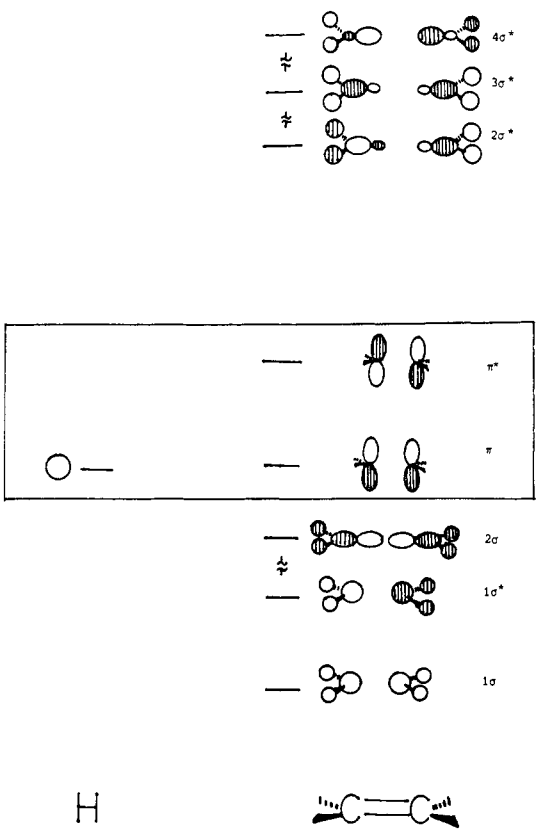

Figure 3. The reactant orbitals which acquire the same symmetry in the complex of H^- and $H_2C{=}CH_2$. The 1s orbital of H is labeled n. The frontier orbitals of the reactants are framed. Hybridization in 1σ $1\sigma^*$ and in 2σ is neglected owing to small s–p mixing.

our description (Tables I–III) of the product state as a resonance hybrid of D^+A^- and D^+A^{-*}:

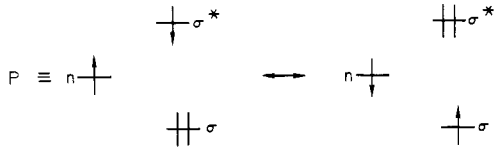

(17)

with an average population of 1 e in n and ~1.5 e each in σ and σ^*. The deviations from these numbers demonstrate the mixing of other excited reactant configurations (especially at the product stage where overlap and hence mixings are large).

When one uses a simple model as a prototype, one must worry whether this model can indeed be applied to more complex systems. Therefore, before we proceed any further, we will attempt to apply the model to a second system. As a test case, we have chosen the reaction between H^- and ethylene (eq 2). This is a more complex problem with more electrons and more orbitals. Not only that, the geometric changes are not as simple. In addition to bond elongations, there are angular deviations which lead to pyramidalization of the trigonal centers of ethylene. Fortunately, this method of analysis can overcome these difficulties. Let us see what they are. The ethylenic moiety has four bonding and four antibonding orbitals which acquire the same symmetry when H^- attacks at one of the carbons, perpendicular to the plane of the molecule. These orbitals are shown in Figure 3. In a MO sense, all of these MOs will mix into each other indirectly via their mixing with n[13], the orbital of the attacking H^-. The orbitals, thus, become unrecognizable so that the main effect, the interaction of the frontier orbitals of the fragments, is masked.

In the reactant-configuration approach, the effect of these additional orbitals is the mixing of other configurations into the main six—*the frontier configurations* of Scheme I. For example, there will be a pack of charge-transfer configurations, $D^+A^-(n \rightarrow \chi^*)$, where one electron is transferred from n to σ^*, $2\sigma^*$, $3\sigma^*$, and $4\sigma^*$, respectively. These can be grouped as one effective, "D^+A^-", configuration, in which that of lowest energy, the frontier reactant configuration $D^+A^-(n \rightarrow \pi^*)$, has the highest weight.[21] The weights of the non-frontier configurations will be significantly smaller, even if the MOs acquire a highly mixed σ–π character. The reason is that the weight of the configurations is the fourth order of reactant-MO coefficients (compare eq 8 and 9). Therefore, although a non-frontier charge-transfer configuration, such as $D^+A^-(n \rightarrow 2\sigma^*)$, contributes to the wave function its contribution will be negligible.

Table V. Coefficients of Reactant Configurations for the Ground Surface, in the Reaction $H^- + H_2C{=}CH_2 \rightarrow H_3C{-}CH_2{}^a$

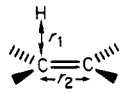

config	coefficients[b,c] R	I	P
DA	1.000	0.432	0.140
$D^+A^-(n \rightarrow \pi^*)$	0.080	0.454	0.380
$DA^*(\pi \rightarrow \pi^*)$	−0.110	−0.272	−0.191
$D^+A^{-*}(n \rightarrow \pi^*, \pi \rightarrow \pi^*)$	−0.006	−0.126	−0.278
$D^+A^-(n \rightarrow 2\sigma^*)$	$<10^{-4}$	0.006	0.004
$D^+A^-(n \rightarrow 3\sigma^*)$	$<10^{-4}$	−0.070	−0.040

[a] The MOs were computed with EH. AO overlap is included. Only Ψ_0 is analyzed. [b] R (r_1 = 3 Å; r_2 = 1.34 Å); I (r_1 = 1.5 Å; r_2 = 1.34 Å); P (r_1 = 1.08 Å; r_2 = 1.5 Å). [c] $|c(n \rightarrow 3\sigma^*)| > |c(n \rightarrow 2\sigma^*)|$ because of the local antisymmetric nature of $2\sigma^*$ with respect to a plane bisecting the C=C bond (Figure 3).

In Table V we show the coefficients of some of the frontier and some of the non-frontier configurations in the ground MO wave function of the complex H^-:··· ethylene. We have chosen three points of interest. In the first, H^-: is placed 3 Å away from the attacked carbon, symbolizing a point close to reactants. In the second point it is 1.5 Å apart, representing a point in the neighborhood of the surface intersection. The final point represents a structure on the product side where the H^-: is only 1.08 Å apart and the C=C bond length is 1.5 Å. The planar geometry of the ethylene was retained throughout.

The resemblence to the H^-: + H_2 problem is evident. Here, too, the ground state starts as a pure DA configuration which almost vanishes at the product state (considering only the Ψ_0 MO wave function). At the same time a pack of excited reactant configurations headed by $D^+A^-(n \rightarrow \pi^*)$ intersects DA, finally becoming the preponderant component in the wave function. As anticipated, the non-frontier configurations play a secondary role. Some representative configurations are listed in Table V and one can see that their contribution is negligible.[22] They are not "needed" for the crossing, but rather they play a role in the geometric relaxation of the olefin.[23,24]

The resemblence to the model system is further illuminated from the inspection of the reactant-orbital populations shown in Table VI.

Only the populations of the frontier reactant orbitals, n, π, and π^*, change significantly as the reaction proceeds. Thus, at the initial point, R, the reaction complex is described mainly by DA, averaging ~2 e in n and ~2 e in π. About the avoided crossing

(21) When one writes "D^+A^-" = $N|D^+A^-(n \rightarrow \pi^*) + \lambda_1 D^+A^-(n \rightarrow 2\sigma^*) + \ldots|$, then, "$D^+A^-$" = $N|| \ldots \pi\bar{\pi}n\bar{\phi}^*| - | \ldots \pi\bar{\pi}\bar{n}\phi^*||$, where $\phi^* = (1 + \lambda_1{}^2 + \ldots)^{-1/2}\{\pi^* + \lambda_1(2\sigma^*) + \ldots\}$. It means that the effective configuration contains a hybridized orbital ϕ^*, which is the π^* orbital mixed with the σ-type orbitals (Figure 3).

(22) Other configurations, $DA^*(2\sigma \rightarrow \pi^*)$ and $D^+A^{-*}(n \rightarrow \pi^*, 2\sigma \rightarrow \pi^*)$, reach maximum values of $c \simeq 0.06$ and $c \simeq 0.02$, respectively.

(23) For example, $D^+A^-(n \rightarrow \pi^*)$ mixes with $D^+A^-(n \rightarrow 2\sigma^*)$ via $2\sigma^*$–π^* mixing (Figure 3). This will increase as the trigonal centers of the olefin are pyramidalized. For MO analysis see: Volland, W. V.; Davidson, E. R.; Borden, W. T. *J. Am. Chem. Soc.* **1979**, *101*, 533–537. Strozier, R. W.; Caramella, P.; Houk, K. N. *Ibid.* **1979**, *101*, 1340–1343.

(24) $D^+A^-(n \rightarrow 2\sigma^*)$ and $D^+A^-(n \rightarrow 3\sigma^*)$ mix with DA via n–$2\sigma^*$ and n–$3\sigma^*$ overlaps. Therefore, another relaxation mode would be the movement of the attacking nucleophile slightly away from the colinear direction above the attacked carbon (see Table V).

Table VI. Electronic Population in the Reactant MOs (RMOs) of the $H^- \cdots H_2C{=}CH_2$ Complex

RMO	population[a,b] R	I	P
n	1.99874	1.42336	0.96233
1σ	2.0000	1.98979	1.94690
$1\sigma^*$	2.0000	1.99043	1.94859
2σ	2.0000	1.99941	1.99708
π	1.99999	1.78796	1.62380
π^*	0.00112	0.78087	1.47804
$2\sigma^*$	0.0000	0.00081	0.00007
$3\sigma^*$	0.00013	0.02078	0.02508
$4\sigma^*$	0.00002	0.00659	0.01810

[a] R, I, and P refer to the three geometries specified in Table V. [b] The frontier RMOs are underlined for clarity.

point, the complex is a resonance hybrid of $D^+A^-(n \rightarrow \pi^*)$ and DA, averaging ~2 e in π, ~1.5 e in n and ~0.5 e in π^* (compare with eq 16 and Table IV). The deviations from these numbers reflect the mixing of the other frontier configurations, e.g., $DA^*(\pi \rightarrow \pi^*)$ and $D^+A^{-*}(n \rightarrow \pi^*, \pi \rightarrow \pi^*)$, which decrease the π population and increase the π^*'s. These configurations mix now more strongly than they did in the model reaction, reflecting that $\pi \rightarrow \pi^*$ excitation is lower than $\sigma_{H-H} \rightarrow \sigma^*_{H-H}$. At the final point, the product-like complex is described by a hybrid of D^+A^- and D^+A^{-*} with smaller mixing of other configurations, thus averaging ~1.5 e in π and in π^* and ~1 e in n (compare with Table IV and eq 17).

The resemblence is not limited to the two reactions discussed so far. It is diagnostic of the type of reaction, one in which while one bond is being broken another is being formed. *Thus, S_N2, nucleophilic aromatic substitution,[6] nucleophilic attacks on carbonyls, proton abstraction by bases, etc., will all exhibit the same type of avoided crossing shown in Figure 1.*

At this stage, one may well ask what other reactions follow this behavior. Therefore, we have decided to search for avoided crossing in reactions involving electrophilic attack,[6c,9] e.g., eq 18 and 19.


(18)

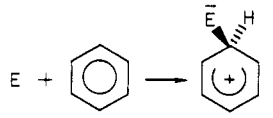
(19)

Here, the substrate (e.g., >C=C<) is the donor, D, and the electrophile, E, is the acceptor, A. As a prototype reaction we have chosen $H^+ + H{-}H \rightarrow H{-}H + H^+$. The configuration analysis in Table VII demonstrate the already recognized pattern. At the initial stage the ground state is DA. At some intermediate point, $DA \leftrightarrow D^+A^-$, and at the final stage it is mainly $D^+A^- \leftrightarrow D^{+*}A^-$ (see footnote *c*, Table VII), where the various configurations are:

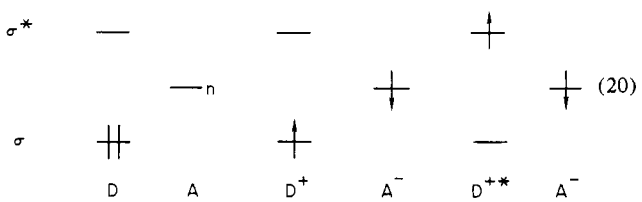
(20)

Once again, we see the same principle at work. As the reaction proceeds an initially excited surface (D^+A^-) is constrained to intersect DA.

This surface intersection *usually* leaves its mark as a thermal barrier on the ground surface (Figure 2). When the surface intersection occurs at very large reactant separation, owing to a very small energy difference between DA and D^+A^- (at infinite D–A separation), the thermal barrier will tend to disappear and the crossing event can only be recognized by analyzing the configurational content of the wave function. In each case the excited surface will be characterized by an energy well at the locus of crossing (see Figure 2 and eq 14 and 15).

Table VII. Coefficients of Reactant Configurations for the Ground Surface of the Model Reaction $H^+ + H_2 \rightarrow H_2 + H^+$

config	coefficients[a-c] R	I	P
DA	1 (0.999)	0.729 (0.640)	0.250 (0.168)
D^+A^-	0 (0.025)	0.604 (0.502)	0.500 (0.350)
$D^{+*}A^-$	0 ($<10^{-3}$)	−0.104 (−0.063)	−0.500 (−0.324)
D*A	0 (-10^{-3})	−0.177 (−0.113)	−0.354 (−0.220)
D**A	0 ($<10^{-3}$)	0.021 (0.010)	0.250 (0.144)
$D^{+2}A^{-2}$	0 ($<10^{-3}$)	0.250 (0.192)	0.500 (0.302)

[a] R, I, and P are the same as in Table I. [b] The coefficients in parentheses are based on EH MOs and the others on neglect of overlap MOs. [c] Note, when the doubly excited MO configurations ϕ_2^2 and ϕ_3^2 are included, the coefficients of D^+A^- and $D^{+*}A^-$ increase and those of the others decrease. For example, at P, the coefficients based on EH MOs will be $c(D^+A^-) \approx (1/(1+\lambda_2^2)^{1/2})\{0.350 + \lambda_2(1.436)\}$, $c(D^{+*}A^-) \approx (-1/(1+\lambda_2^2)^{1/2})\{0.324 + \lambda_2(1.491)\}$, and $c(D^{+2}A^{-2}) \approx (1/(1+\lambda_2^2)^{1/2})\{0.302 - \lambda_2(1.346)\}$.

The avoided surface crossing just discussed covers quite a range of organic reactions, comprising of both nucleophilic and electrophilic attack. Therefore, at this point we will digress somewhat and try to clarify the reason for this topological behavior.

II. Crossing of VB Structures

What is the intimate nature of the surface intersection just described? Why must it occur during the chemical transformation? Some insight into the answers can be gained if we return to Scheme I. We start the reaction with a wave function which is mainly DA. In this configuration, the acceptor A has a bond represented by two electrons in a bonding orbital (a bond pair) and there is no bond between D and A. In D^+A^- there are two spin-paired electrons—one on D^+ (in n) and the other on A^- (in χ^*). These spin-paired electrons constitute the bond pair which will be responsible for D–A bonding. Together with this, the bond in A is being weakened, since one electron resides now in an antibonding orbital χ^*. Thus, the $DA{-}D^+A^-$ intersection reflects the electronic reshuffle—breaking of an old bond (in A) and formation of a new one (between D and A).

In order to see that more clearly, we must examine the original VB ideas put forward some decades ago.[25,26] Imagine a covalent bond forming between two atomic centers M and N, each having one orbital (or hybrid). The principal configuration which describes the union is the so-called "covalent" or diradicaloid $(\phi_M^1\phi_N^1)$[17] Heitler-London type wave function:

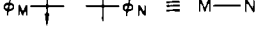
(21)

There are two more configurations, ϕ_M^2 and ϕ_N^2, with smaller weights. These are called zwitterionic[17] and their importance increases as the M–N bond becomes more polar.[27] These features

(25) The origins of VB theory can be traced back all the way to Heisenberg. It was applied first by Heitler and Londong to H_2. Its generalized form was formulated by Hurley, Lennard-Jones, and Pople: (a) Heisenberg, W. *Z. Phys.* **1926**, *38*, 411. *Ibid.* **1926**, *39*, 499. *Ibid.* **1927**, *41*, 239. (b) Heitler, W.; London, F. *Ibid.* **1927**, *44*, 455. (c) Hurley, A. C.; Lennard-Jones, J. E.; Pople, J. A. *Proc. R. Soc. London, Ser. A* **1953**, *A220*, 446.

(26) For other sources of VB computations and ideas see: (a) van der Lugt, W. Th. A. M.; Oosterhoff, L. J. *Mol. Phys.* **1970**, *18*, 177–190. (b) van der Hart, W. J.; Mulder, J. J. C.; Oosterhoff, L. J. *J. Am. Chem. Soc.* **1972**, *94*, 5724–5730. (c) Campion, W. J.; Karplus, M. *Mol. Phys.* **1973**, *25*, 921–936. (d) Reference 11a. (e) Harcourt, R. D. *J. Am. Chem. Soc.* **1978** *100*, 8060–8062 and references cited therein. (f) Halgren, T. A.; Brown, L. D.; Kleir, D. A.; Lipscomb, W. N. *Ibid.* **1977**, *99*, 6793–6806. (g) Matsen, F. A. *Acc. Chem. Res.* **1978**, *11*, 387–392.

(27) In the GVB formalism (ref 11a), a bond pair is described in a Heitler-London type wave function, using slightly delocalized AOs χ_M and χ_N, so that: $2^{-1/2}[\chi_M\chi_N + \chi_N\chi_M] = \Psi_{COV} + \lambda\Psi_{ION}$, where λ is related to the degree of delocalization of the generalized AOs χ_M and χ_N.

are retained even when one talks about most covalent bonds which are not as strictly localized as that in H_2.[27] In each case, one finds a heavy weight of the diradicaloid VB structure (eq 21) with high amplitudes on atomic orbitals or hybrids of the union centers. Since the covalent structure (eq 21) is the major contribution to most covalent bonds, we will concentrate, for simplicity, on this structure in our further discussions.

Let us go back now and interpret the DA–D^+A^- crossing in VB terms. As an example, where such crossing occurs, we choose the nucleophilic addition of a nucleiphile X: to an unsaturated system, >C=Y, where Y is a more electronegative group than C. We can expand the reactant configurations into VB structures in exactly the same manner used to expand MO wave functions into reactant configurations (see supplementary material).

We have shown before that only frontier configurations are needed to describe the crossing event, whereas the non-frontier configurations effectively hybridize the frontier orbitals via $\sigma-\pi$ mixing (Table V).[23] Thus, we can focus on the frontier oritals shown in eq 22, keeping the hybridization effect in mind.

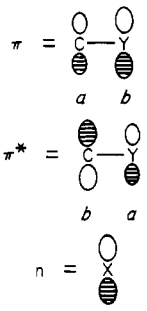

(22)

$|b| > |a|, a^2 + b^2 = 1$

Using the notations in eq 22, we find that at the reaction starting point, where the system is described by DA mixed mainly with some DA**, the major VB structure[17,28] which describes the system is

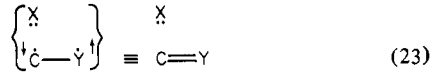

(23)

This structure has two spin-paired electrons (indicated by arrows) which describe the original π bond in the reactant >C=Y in analogy with the description of a bond in eq 21. We recall that this bond has to be cleaved during the reaction and replaced by a new bond between X and C. Therefore, we understand that this VB structure has to vanish from the wave function at the reaction final point and be replaced by another—one which describes the newly formed bond X–C.

Let us see which configuration is the one containing the latter VB structure. Using eq 22, we obtain:

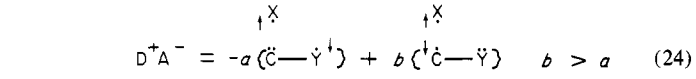

(24)

The major VB structure in eq 24 is the desired one having two spin-paired electrons—one on C and one on X. Thus, D^+A^- contains as a major contribution, the VB structure which describes the newly formed bond X–C[28] on account of the old $\pi_{C=Y}$ bond which is being cleaved.

This is the reason behind the avoided crossing which we described in section I in terms of two principal configurations DA and D^+A^-. The avoided crossing describes nothing else but the fact that one bond is breaking and is being replaced by a new one. Without this crossing, the bond shift, and hence product formation, does not take place.

(28) Using the notations in eq 22, we have reached the following results: $DA - \lambda DA^{**} = \sqrt{2}ab(1 + \lambda)\{X{:}\,\dot{C}{-}\dot{Y}\} + (a^2 - \lambda b^2)\{X{:}\,\ddot{C}{-}Y\} + (b^2 - \lambda a^2)\{X{:}\,C{-}\ddot{Y}\}$; $DA^* = (a^2 - b^2)\{X{:}\,\dot{C}{-}\dot{Y}\} + \sqrt{2}ab\{X{:}\,\ddot{C}{-}Y \leftrightarrow X{:}\,C{-}\dot{Y}\}$; $D^{+2}A^{-2} = \{X\ddot{C}{-}\dot{Y}\}$. Thus, the zwitterionic components of the two bonds in question are provided by DA*, DA**, and $D^{+2}A^{-2}$.

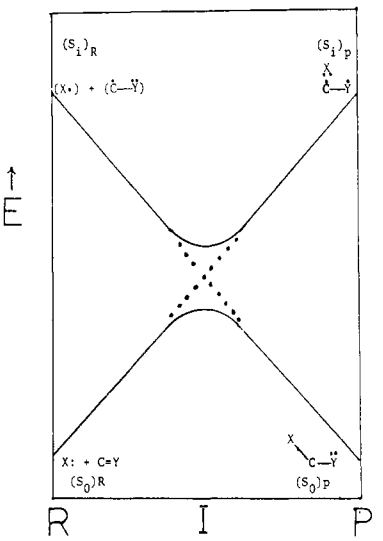

Figure 4. Schematic representation of the curve crossing in nucelophilic attack. R, I, and P are reactant, intermediate, and product geometries, respectively. The crossing is shown with the use of the two main VB structures *only*; one describes the initial ground state, $(S_0)_R$, and the other describes an initial excited state, $(S_i)_R$. Other VB structures are omitted for clarity. The single dots on adjacent atoms indicate odd electrons which are spin coupled. No thermodynamic information is implied in descrbing the reactants and products.

This is where we would like to digress and clarify our previous remark (section I) that the D–A formalism (although geared toward thinking about reactions in the forward direction) only seemingly treats the forward and the reverse reactions differently. At the product stage, the wave function is described mainly by a mixture of D^+A^- and D^+A^{-*}. D^+A^{-*} is shown in eq 25.

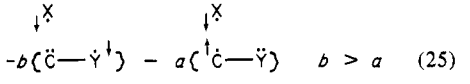

(25)

Taking the negative linear combination of D^+A^- (eq 24) and D^+A^{-*}, we get:

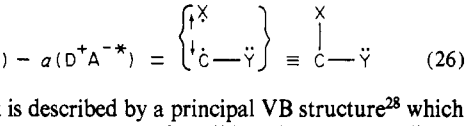

(26)

Thus, the product is described by a principal VB structure[28] which is analogous to the VB structure describing the reactants (in eq 23), the two differing only by a bond shift. Therefore, the D–A formalism treats the forward and the reverse reactions on an equal basis, though this is not evident from the configurations themselves. It becomes clear only by inspecting the corresponding VB structures.

Now that we have interpreted the avoided crossing in VB terms, we understand that this is actually a mechanism whereby the reactants (X: and >C=Y) rearrange their electrons, so that an old bond ($\pi_{C=Y}$) will be replaced by a new bond (X–C). Thus, if we choose to focus *only* on the main VB structures, we can describe the avoided crossing in a schematic and a simplified manner as a crossover of two VB forms—one describing the old bond and the other the newly formed bond.[29] This is done in Figure 4 for the nucleophilic attack discussed before.

Returning to reactant configurations, we understand now why D^+A^- was selected to cross DA during the chemical transformation. *In this configuration, the reactants are prepared for bonding, having odd electrons in their union centers, and, hence, they can be coupled to form the new bond.*

As we shall see immediately, this principle does not only apply to nucleophilic and electrophilic reactions. Its ramifications are considerably wider and apply *whenever at least one of the reactants is closed shell.* Whenever both reactants are open shell, such as

(29) Similar interpretation of S_N2 transition state is given in ref 7c.

in radical recombination (e.g., $2H\cdot \rightarrow H_2$), the reaction involves only bond making; *the two reactants are already prepared for bonding*, so that crossing does not occur. In other words, in such cases, the reaction surface can be described throughout mainly by a single VB structure or reactant configuration.

III. The Role of Symmetry

Until now we have not imposed any symmetry constraints on the reactions. The avoided crossing was found to owe its nature to the selection of the "right" reactant configurations needed to partake in the bonding reorganization process. Consequently, the open-shell reactant configuration, D^+A^-, was selected to initiate the crossover, since it involves odd electrons, one on each fragment, which can be coupled to form the new bond. What happens then when the odd electrons are in orbitals which do not have a symmetry match? This will be the case when, for example, the nucleophile will attack at the center, such as:

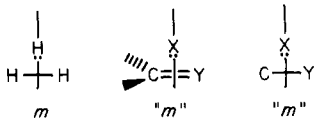

(27)

Now, the D^+A^- configuration will not be effective in initiating the new bond since it places the two odd electrons in oritals (n and σ^*) which do not have a symmetry match (S and A with respect to the plane *m* or the pseudo-plane "*m*"). On the other hand, D^+A^{-*} has the odd electrons in orbitals which have a symmetry match, as shown in eq 28 for H_3^-. Consequently,

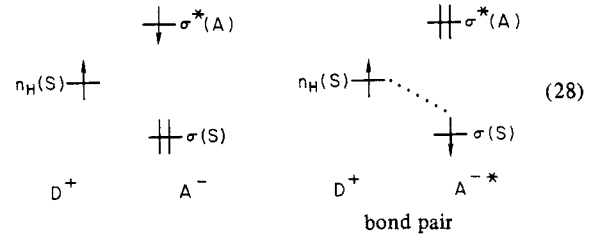

(28)

D^+A^{-*}, heading the pack of the diexcited reactant configurations, will be selected to cross DA, while D^+A^- will remain an excited state. This is the well-known surface crossing in the Longuet-Higgins–Abrahamson[2] and Woodward-Hoffmann[3] correlation diagrams. Thus, what symmetry will do is simply to select from the open shell excited configurations the ones which can form the new bonds.

Let us see that this indeed is the case. The molecular orbitals of the cyclic H_3^- complex (eq 27) can be expressed, with neglect of overlap, as:

$$\phi_1 = an_H + b\sigma \qquad \phi_2 = -bn_H + a\sigma \qquad \phi_3 = \sigma^*$$
$$a^2 + b^2 = 1 \tag{29}$$

Expansion of the MO wave function $\phi_1^2\phi_2^2$ shows that it contains only DA. Hence, it cannot define the product. The doubly excited MO configuration, $\phi_1^2\phi_3^2$, which crosses to define the product in the Woodward–Hoffmann and Longuet-Higgins–Abrahamson diagrams, yields:

$$\phi_1^2\phi_3^2 = b^2D^{+2}A^{-2} + a^2DA^{**} + \sqrt{2}abD^+A^{-*} \tag{30}$$

At the locus of MO crossing,[1] $a = 1/\sqrt{3}$ and $b = (2/3)^{1/2}$, hence, $\phi_1^2\phi_3^2 = {}^2/_3D^{+2}A^{-2} + {}^1/_3DA^{**} + {}^2/_3D^+A^{-*}$. Past the crossing point, the coefficient *a* increases, while *b* decreases, i.e., $a > 1/\sqrt{3}$ while $b < 2/\sqrt{3}$ and, hence, D^+A^{-*} becomes the leading configuration. Inclusion of the other doubly excited state $\phi_2^2\phi_3^2$ which mixes into $\phi_1^2\phi_3^2$ with a negative sign, via bielectronic parts of the hamiltonian,[16] further increases the coefficient of D^+A^{-*} and decreases those of $D^{+2}A^{-2}$ and DA^{**}, making the former the leading configuration:

$$\phi_1^2\phi_3^2 - \lambda\phi_2^2\phi_3^2 =$$
$$(b^2 - \lambda a^2)D^{+2}A^{-2} + (a^2 - \lambda b^2)DA^{**} + \sqrt{2}ab(1 + \lambda)D^+A^{-*} \tag{31}$$

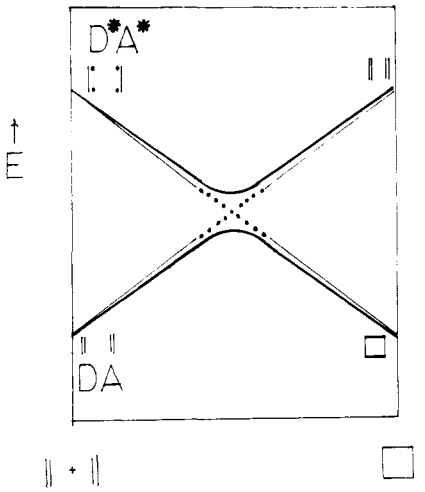

Figure 5. Schematic representation of the curve crossing in the forbidden reaction of two olefins, one labeled D and the other A. The thick lines are the adiabatic curves. The avoided crossing (a bielectronic effect in this case) is indicated by circles. The single dots on the olefins indicate odd electrons which are spin uncoupled on each olefin but are coupled across the reaction centers. This state (D*A*) leads to formation of two new bonds as the olefins approach one another. No thermodynamic information is implied in describing the reactants and products.

As we have said before, symmetry does not affect the intimate nature of the avoided crossing. It only determines which of the open shell excited configurations possess the odd electrons in orbitals which have a symmetry match and, hence, can intersect DA to define the products.

The generality of this surface crossing rule can be further brought into focus by the well-known example of forbidden $\pi 2_s + \pi 2_s$ cycloadditions. Others[5a,c-g] as well as we[6c] have concluded that the avoided crossing in the reaction of two olefins, D and A, arises primarily from the intersection of the no-bond DA with doubly excited configurations $^1(D^{*3}A^{*3})$, in which two triplet ethylenes are coupled into a singlet as shown in eq 32 which show

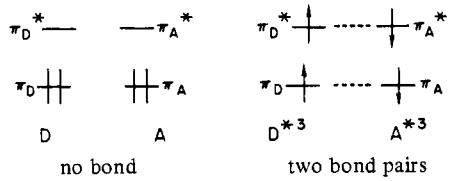

(32)

that there are two pairs of odd electrons to form the new bonds, and each bond pair electron resides in orbitals having a symmetry match.

In VB terms, triplet $\pi\pi^*$ is the purely covalent structure $\{\uparrow \dot{C}—\dot{C}\uparrow\}$.[17a,b] Thus, the VB description of the DA–$^1(D^{*3}A^{*3})$ crossing is simply:[30]

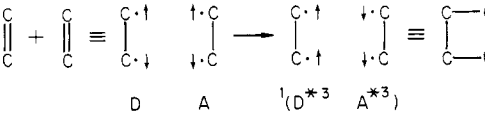

(33)

Once again we see that the configuration which is selected to cross DA contains odd unpaired electrons on the reaction centers, ready for bond making.[31] The avoided crossing is, thus, merely

(30) There are also zwitterionic components which are contributed as $D^{*3}A^{*3}$ is being spin adapted to a singlet, i.e.: $^1(D^{*3}A^{*3}) = N\{|\pi_D\pi_D^*\bar{\pi}_A\bar{\pi}_A^*| + |\bar{\pi}_D\bar{\pi}_D^*\pi_A\pi_A^*| - |\pi_D\bar{\pi}_D^*\bar{\pi}_A\pi_A^*| - |\bar{\pi}_D\pi_D^*\pi_A\bar{\pi}_A^*|\}$. There are other contributions to the wave function of the product, e.g., D^+A^{-*}, $D^{-*}A^+$, $D^{+*}A^-$, D^-A^{+*}, $D^{+2}A^{-2}$, and $D^{-2}A^{+2}$. See discussion in ref 6c.

(31) An analogous reaction is formation of ethylene from two carbenes. Ethylene can be described as two triplet carbenes coupled to a singlet: $(H_2\dot{C}\cdot\cdot\dot{C}H_2) \equiv H_2C{=}CH_2$. See: Cheung, L. M.; Sundberg, K. R.; Ruedenberg, K., *J. Am. Chem. Soc.* **1978**, *100*, 8024–8025. As noted by the authors, no barrier appears on the reaction surface. This results from the fact that the surface is described throughout by one major configuration.

an intersection of two VB structures, one describing the old bonds the other the new bonds.

These considerations are illustrated in Figure 5 and the resemblence to the case in Figure 4 is obvious. Thus, the roots of avoided crossing are topologically invariant. Avoided crossing arises whenever the reactants (or at least one of them) are closed shell. Therefore, in order to effect bonding reorganization, the no-bond configuration, DA, must be replaced by another configuration in which the reactants are prepared for bonding. The configuration which crosses over is initially the lowest excited reactant configuration that contains, per each new bond, two odd electrons which are spin paired (a bond pair) and which reside in reactant orbitals having a symmetry match (e.g., D^+A^-, D^*A^*, etc.). Alternatively, this crossing can be viewed as an interchange of two VB structures—one reactant-like and the other product-like (Figures 4 and 5).

IV. Conclusions

We have asked at the outset: what happens to molecules as they react? Now we have an answer. When closed shell reactants D and A are transformed to products they undergo a change in their valence shell. For example, in nucleophilic and electrophilic attacks, the initial changes are $D \rightarrow D^+$, and $A \rightarrow A^-$. The same changes in the forbidden reaction[1-3] of two olefins are $D \rightarrow D^{*3}$ and $A \rightarrow A^{*3}$. These changes prepare the reactants for bonding by placing odd electrons at their reaction centers. *As long as the reactants do not reach this prepared valence state, bonding changes are only slight and any adduct that will form is merely a loose association complex, one in which the reactants retain their electronic and structural integrity.*

The preparation of the reactants for bonding can be related to the heuristic process of promotion discussed in any organic chemistry textbook for atoms. Since the reactants (*or at least one of them*) start as closed shell entities they must be transformed to open shell entities in order to create new bonds and break old ones. For example, in nucleophilic reactions,

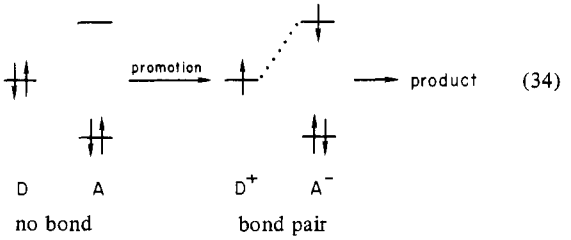

(34)

In other words, the promotion necessary for preparing the reactants for bonding is brought about via the intersection of DA by an excited surface which contains the "image" of the product.

Our second and related question was: what is the mechanism of barrier formation in organic reactions? Barriers are formed because reactants have to open their valence shells and be prepared for bonding before they can be transformed to products. Therefore, they must climb up in energy until the "right" excited configuration descends sufficiently in energy so that the system crossover and roll down to product. By "right" we mean the lowest excited reactant configuration which contains a bond pair (i.e., two spin-paired electrons) per each new bond, in orbitals having a symmetry match (see eq 28).

The height of the barrier depends on the initial energy gap between DA and the excited reactant configuration which crosses it, and on the degree of their avoided crossing. For example, the height of the barrier for all nucleophilic and electrophilic attack depends on the difference between the ionization energy of the donor (I_D) and the electron affinity of the acceptor (A_A), while that for forbidden 2 + 2 reactions depends on the sum of the triplet energies of D and A.[6e]

What rests behind the avoided crossing is the intimate nature of the chemical transformation—a changeover of bonds. Therefore, we believe that our conclusions should carry over to other classes of organic reactions which involve at least one closed shell reactant, such as radical additions, rearrangements, symmetry allowed reactions, etc.[32] Whenever both reactants are open shell (e.g., radical recombination) no crossing occurs[31] and the entire reaction surface will be described mainly by one reactant configuration or a VB structure.[33]

With this we end on a general note. We have taken the reader in a most circuituous manner all the way from adiabatic MO–CI electronic curves to their intimate VB components. Then we found that a wide range of potential energy curves can be described as arising from the intersection of two VB structures—something which is intuitively conveyed in the electron-pushing mnemonics used to describe mechanisms of organic reactions, e.g.,

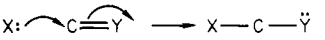

(35)

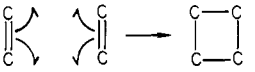

(36)

Was it necessary to take this path? Could we not simply start from a VB treatment? Yes, one could in principle skip all the steps and construct the surface, for instance, for the linear nucleophilic reaction $H^- + H_2 \rightarrow H_2 + H^-$ directly from the VB structures with H: $H^{\uparrow}\cdot\cdot^{\downarrow}H$ and $H^{\downarrow}\cdot\cdot^{\uparrow}H$:H being the main forms (with minor contributions from the rest, e.g., H: H :H and $H^{\uparrow}\cdot$ H: $\cdot^{\downarrow}H$), much the same as we did in Figure 4. However, we believe the insight which is gained by the chemically more transparent D–A approach would have been lost in the process. For example, what is the relationship between reaction rates and physical quantities of the reactants, such as the ionization energy of the donor (I_D), the electron affinity of the acceptor (A_A), and their excitation energies? What kind of distortions do the reactants experience as the reaction complex proceeds toward the products? Is the transition state "tight" or is it "loose"? All these can be exposed more readily by the combined power of analysis of the three methods: MO approach, D–A approach, and VB theory. Some of the applications will be treated in the future.

Acknowledgment. The author is indebted to Dr. A. Pross for many enlightening comments.

Supplementary Material Available: An appendix which summarizes the algorithms for projecting configurations and VB structures out of delocalized MOs, and for evaluating matrix elements of configurations and of VB forms (8 pages). Ordering information is given on any current masthead page.

(32) We already have the results for the cleavage of H_2 by H^+ through a symmetry-allowed cyclic structure. Here too, D^+A^- and $D^{+*}A^-$ intersect DA. We are investigating now the Diels–Alder reaction. Recent results by Houk and his co-workers indicate that such crossing occurs also in symmetry-allowed reactions; see: Houk, K. N.; Gandour, R. W.; Strozier, R. W.; Rondan, N. G.; Paquette, L. A., *J. Am. Chem. Soc.* **1979**, *101*, 6797–6802. Other preliminary results show surface crossing for radical attacks, and 1,2 rearrangements. For example, in the radical attack $H\cdot + H_2 \rightarrow H_2 + H\cdot$, the excited surface that crosses $^2DA(H\cdot H_2)$ is $^2(DA^{*3})[H\cdot H_2(^3\sigma\sigma^*)]$.

(33) Note that the conclusions do not apply to ionic bonds. When one deals with ionic bonds many conclusions are altered. For example, atom combination involves surface crossing of the covalent–ionic type such as the one accompanying the formation of NaCl (see, for example, ref 5*l*).